Inorg. Chem. **2004**, *43*, 7902–7915

Forum

Understanding Metalloprotein Folding Using a de Novo Design Strategy

Debdip Ghosh and Vincent L. Pecoraro*

Department of Chemistry, University of Michigan, Ann Arbor, Michigan 48109-1055

Received August 3, 2004

Metal ions play significant roles in most biological systems. Over the past two decades, there has been significant interest in the redesign of existing metal binding sites in proteins/peptides and the introduction of metals into folded proteins/peptides. Recent research has focused on the effects of metal binding on the overall secondary and tertiary conformations of unstructured peptides/proteins. In this context, de novo design of metallopeptides has become a valuable approach for studying the consequence of metal binding. It has been seen that metal ions not only direct folding of partially folded peptides but have at times also been the elixir for properly folding random-coil-like structures in stable secondary conformations. Work in our group has focused on binding of heavy metal ions such as Hg(II) to de novo designed α-helical three stranded coiled coil peptides with sequences based on the heptad repeat motif. Removal from or addition of a heptad to the parent 30-residue TRI peptide with the amino acid sequence Ac-G(LKALEEK)$_4$G-NH$_2$ generated peptides whose self-aggregation affinities were seen to be dependent on their lengths. It was noted that adjustment in the position of the thiol from an "*a*" position in the case of the shorter BabyL9C to a "*d*" position for BabyL12C resulted in a peptide with low association affinities for itself, weaker binding with Hg(II), and a considerably faster kinetic profile for metal insertion. Similar differences in thermodynamic and kinetic parameters were also noted for the longer TRI peptides. At the same time, metal insertion into the prefolded and longer TRI and Grand peptides has clearly demonstrated that the metal binding is both thermodynamically as well kinetically different from that to unassociated peptides.

Introduction

The problem of metalloprotein folding can be studied by the preparation of peptides crafted using first principles in the hope of generating "functionally active" biomolecules.[1−3] This design strategy involves the construction of a peptide intended to fold into a precisely defined three-dimensional structure, with a sequence that is not derived from that of any natural protein.[4] For the most part, de novo design has followed a minimalist approach to design the peptidic scaffold.[5,6] The advantage of this approach is that specific structure types can be ascertained without the complication of deconvoluting the behavior of multiple alternate folding domains present in natural systems. In general, there is still a serious lack of knowledge describing the relationship between the peptidic backbone sequence, its secondary and tertiary structures, and the functional properties of the protein. A survey of the literature suggests that reports detailing metal-induced protein folding are sparse. This observation is remarkable given that it is estimated that one-third of proteins contain metals which are indispensable for proper function.

Significant attention has focused on engineering metal binding sites in de novo designed peptides because of the importance of metals in biology. The rate of research in the

* To whom correspondence should be addressed. E-mail: vlpec@umich.edu.

(1) Lombardi, A.; Summa, C. M.; Geremia, S.; Randaccio, L.; Pavone, V.; DeGrado, W. F. *Proc. Nat. Acad. Sci. U.S.A.* **2000**, *97*, 6298−6305.
(2) Hill, R. B.; Raleigh, D. P.; Lombardi, A.; DeGrado, W. F. *Acc. Chem. Res.* **2000**, *33*, 745−754.
(3) Nastri, F.; Lombardi, A.; Pavone, V. *Chem. Rev.* **2001**, *101*, 3165−3189.
(4) DeGrado, W. F.; Summa, C. M.; Pavone, V.; Nastri, F.; Lombardi, A. *Annu. Rev. Biochem.* **1999**, *68*, 779−819.
(5) DeGrado, W. F.; Wasserman, Z. R.; Lear, J. D. *Science* **1989**, *243*, 622−628.
(6) Bryson, J. W.; Betz, S. F.; Lu, Z. X.; Suich, D. J.; Zhou, H. X. *Science* **1995**, *270*, 935−941.

10.1021/ic048939z CCC: $27.50
Published on Web 10/28/2004

field of metallopeptide design has seen a tremendous jump in the past few years resulting in the emergence of very distinct approaches. The focus of this article will primarily be on those studies that are helpful in clarifying how metal ions can assist or direct peptide folding. Interested readers should consult some very pertinent reviews[7−21] in order to obtain a broader overview of the metalloprotein design field. In the review portion of this article, the binding of metals to de novo designed peptides has been discussed under the following categories: (1) metal assisted folding of unstructured/partially structured de novo designed α-helices, (a) enhancement of α-helical character in partially folded peptides, (b) metal induced folding of random coils to generate α-helices; (2) metal binding to folded de novo designed proteins/peptides, (a) metal binding to folded α-helical peptides, (b) metal binding to β-turns and β-sheets.

This presentation will center primarily on metal induced folding of unstructured and partially structured peptides.

(1) Metal Assisted Folding of Unstructured/Partially Structured de Novo Designed α-Helices

The minimalist approach to de novo peptide design gives rise to proteins that are generally much simpler than the natural proteins that they are mimicking, yet poses sufficient complexity in structure both for studying the folding as well as the functional properties. The most commonly used *de novo* designed structural motif is the α-helix and in general α-helical coiled coils. An α-helical coiled coil consists of two, three, or four amphipathic α-helices that often contain a seven amino acid "heptad repeat" denoted by the letters *abcdefg*. Hydrophobic residues that are placed at the "*a*" and "*d*" positions are directed into the core of the protein. The properties of an α-helix orient the "*a′*" residue, the first of the subsequent heptad to be arranged almost directly below the "*a*" residue. The "*a*" and "*a′*" residues are actually 20° out of phase, leading to α-helices that twist around each other to form a coiled coil. Hydrophilic residues are placed at "*b*", "*c*", "*e*", and "*g*" positions. These residues assist in inter-helical electrostatic interactions which can orient the helices in parallel or antiparallel configurations. A helical wheel diagram that illustrates these interactions for parallel oriented coiled coils is given as Figure 1.

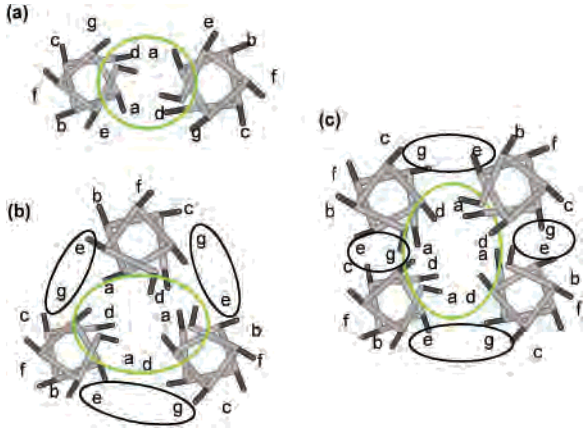

Figure 1. Helical wheel diagram for parallel two, three, and four stranded coiled coil peptides.

(a) Enhancement of α-Helical Character in Partially Folded Peptides. Significant effort has been expended studying binding of metals to partially folded peptides to influence their secondary conformations.[22−29] Among the earliest contributions in this field was the work of Ghadiri et al. who designed two 15-mer peptides with the sequence Ac-AEAAAKEAAALX$_1$AAAX$_2$A-NH$_2$, replacing the X-residues with two histidine residues in one peptide and one cysteine and one histidine in the other.[30] Binding of these peptides with Cd(II), Cu(II), Ni(II), and Zn(II) were followed using circular dichroism and showed metal-ion selective binding dependent on the affinity of the metal ions for the ligands. In every case, however, enhancements in the helix content of the peptides were observed on their consequent binding to the metal ions. To further the scope of studying systems under suitable physiological conditions, an exchange-inert metallopeptide system was designed,[31] showing the binding of Ru(III) to two peptidic systems. For both peptides, helical characters of the peptides were seen to increase on metal ion complexation. To further increase the role of the metal ion as a cross-linking agent, the bipyridine moiety has often been used as a ligand to bind the metal.[32−34] Using the same principle, a 15-mer peptide (Bipy-GELAQKLEQALQK-LA) was designed containing a 5-carboxy-2,2′-bipyridine

(7) Findlay, W. A.; Shaw, G. S.; Sykes, B. D. *Curr. Opin. Struct. Biol.* **1992**, *2*, 57−60.
(8) Berg, J. M. *Curr. Opin. Struct. Biol.* **1993**, *3*, 585−588.
(9) Regan, L. *Trends Biochem. Sci.* **1995**, *20*, 280−285.
(10) Hellinga, H. W. *Curr. Opin. Biotechnol.* **1996**, *7*, 437−441.
(11) Tuchscherer, G.; Dumy, P.; Mutter, M. *Chimia* **1996**, *50*, 644−648.
(12) Lu, Y.; Valentine, J. S. *Curr. Opin. Struct. Biol.* **1997**, *7*, 495−500.
(13) Regan, L. *Adv. Mol. Cell Biol.* **1997**, *22A*, 51−80.
(14) Hellinga, H. W. *Folding Des.* **1998**, *3*, R1−R8.
(15) Benson, D. R.; Wisz, M. S.; Hellinga, H. W. *Curr. Opin. Biotechnol.* **1998**, *9*, 370−376.
(16) Cox, E. H.; McLendon, G. L. *Curr. Opin. Chem. Biol.* **2000**, *4*, 162−165.
(17) Xing, G.; DeRose, V. J. *Curr. Opin. Chem. Biol.* **2001**, *5*, 196−200.
(18) Kennedy, M. C.; Gibney, B. R. *Curr. Opin. Struct. Biol.* **2001**, *11*, 485−490.
(19) Lu, Y.; Berry, S. M.; Pfister, T. D. *Chem. Rev.* **2001**, *101*, 3047−3080.
(20) Baltzer, L.; Nilsson, J. *Curr. Opin. Biotechnol.* **2001**, *12*, 355−360.
(21) Barker, P. D. *Curr. Opin. Struct. Biol.* **2003**, *13*, 490−499.
(22) Ruan, F.; Chen, Y.; Hopkins, P. B. *J. Am. Chem. Soc.* **1990**, *112*, 9403−9404.
(23) Ruan, F.; Chen, Y.; Itoh, K.; Sasaki, T.; Hopkins, P. B. *J. Org. Chem.* **1991**, *56*, 4347−4354.
(24) Cheng, R. P.; Fisher, S. L.; Imperiali, B. *J. Chem. Soc., Dalton Trans.* **1996**, *118*, 11349−11356.
(25) Impellizzeri, G.; Pappalardo, G.; Purello, R.; Rizzarelli, E.; Santoro, A. M. *Chem.—Eur. J.* **1998**, *4*, 1791−1798.
(26) Henin, O.; Barbier, B.; Boillot, F.; Brack, A. *Chem.—Eur. J.* **1999**, *5*, 218−226.
(27) Cline, D. J.; Thorpe, C.; Schneider, J. P. *J. Am. Chem. Soc.* **2003**, *125*, 2923−2929.
(28) Spiga, O.; Scarselli, M.; Bernini, A.; Ciutti, A.; Giovannoni, L.; Laschi, F.; Bracci, L.; Niccolai, N. *Biophys. Chem.* **1997**, *97*, 79−86.
(29) Spiga, O.; Bernini, A.; Scarselli, M.; Ciutti, A.; Giovannoni, L.; Laschi, F.; Bracci, L.; Niccolai, N. *J. Pept. Sci.* **2002**, *8*, 634−641.
(30) Ghadiri, M. R.; Choi, C. *J. Am. Chem. Soc.* **1990**, *112*, 1630−1632.
(31) Ghadiri, M. R.; Fernholz, K. *J. Am. Chem. Soc.* **1990**, *112*, 9633−9635.
(32) Lieberman, M.; Sasaki, T. *J. Am. Chem. Soc.* **1991**, *113*, 1470−1471.
(33) Lieberman, M.; Tabet, M.; Sasaki, T. *J. Am. Chem. Soc.* **1994**, *116*, 5035−5044.
(34) Mutz, M. W.; McLendon, G. L.; Wishart, J. F.; Gaillard, E. R.; Corin, A. F. *Proc. Natl. Acad. Sci. U.S.A.* **1996**, *93*, 9521−9526.

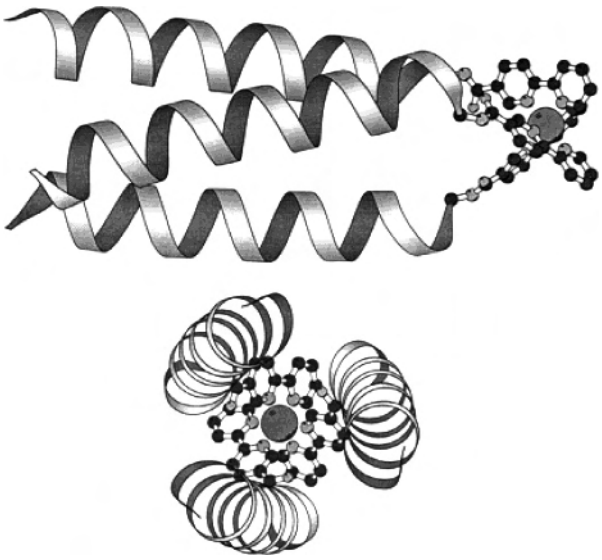

Figure 2. Molscript model of Δ-*fac*-$[Ru(P_20)_3]^{2+}$ viewed from above and from the side. The ruthenium tris-bipyridyl moiety is shown in ball-and-stick-representation. The figure is taken from the following reference: Case, M. A.; Ghadiri, M. R.; Mutz, M. W.; McLendon, G. L. Stereoselection in designed three-helix bundle metalloproteins. *Chirality* **1998**, *10*, 35−40. Copyright 1998, Wiley-Liss Inc. Reprinted by permission of Wiley-Liss Inc., a subsidiary of John Wiley & Sons, Inc.

moiety at the N-terminus.[35] In the absence of a metal ion, the peptide was monomeric showing ∼30% helicity; however, the peptide spontaneously self-assembled into a 45-residue triple-helical metalloprotein displaying ∼65% helicity upon addition of transition metal ions such as Ni(II), Co(II), or Ru(II). This triple helical metalloprotein was further used as a starting material for the rational design of a heterodinuclear Ru(II)Cu(II) metalloprotein.[36] In a separate work, Ghadiri et al. designed a 15-mer peptide having a pyridyl moiety at the N-terminal which self-assembled in the presence of Ru(II) to form a four-helix bundle metalloprotein.[37]

An interesting stereochemical study examined the assembly of an eicosameric peptide (P_{20}) having 20 residues and a similar 5-carboxy-2,2′-bipyridyl group at the N-terminus.[38] It was expected that binding of a transition metal to the bipyridine moiety would yield an octahedral $[M(bpy)_3]^{n+}$ complex. This geometry was expected to influence the resulting topology of the three-helix peptidic bundle. A smaller bipyridyl tripeptide (P_3) containing the first three residues of the longer 20-mer peptide was also synthesized. The Ru(II) complex of P_3 was used as a standard to assess the influence of secondary and tertiary conformations of the longer peptide on the final stereochemistry of the complex. While P_3 led solely to a racemic mixture of four possible diastereomers Δ-*mer*/Λ-*mer*/Δ-*fac*/Λ-*fac* in the ratio 3:3:1:1, the longer peptide P_{20} (Figure 2) showed an unexpected bias in excess of 80% for the disfavored *fac*-diastereomers over the more probable *mer*-conformers. This preference was attributed to the formation of a parallel coiled coil which induced selection of the facial isomers in which all three chains were expected to propagate from the same face of the coordinating octahedron. This study was believed to be the first report of stereoselection of such a magnitude for a system under kinetic control. Further work on this peptide was pursued by altering the sequence backbone[39,40] by deletion of a single hydrogen bond; however, this modification did not seem to perturb the secondary conformations, even though the overall folding free energy was seen to decrease. Nuclear magnetic resonance spectroscopic studies of the peptides with various paramagnetic metal ions[41] like Ni(II) and Co(II) showed the presence of a dual conformation for the bundle up to the 12th residue from the N-terminus, displaying two different facial isomers with distinct susceptibility tensors. The structures of both the isomeric forms were ascertained from interpretation of the nuclear Ovehauser effects of the Ni(II) complex and ^1H pseudocontact shifts of the Co(II) complex.

Often, groups have modified metal binding sites of naturally occurring proteins to create a new class of peptides incorporating functional attributes of more than one native sequence. Franklin et al. have designed a 33-mer peptide comprising helices α2 and α3 of a helix−turn−helix DNA-binding motif protein and introduced the EF-hand Ca-binding loop as the turn in the sequence as shown in Figure 3. This chimera P3 bound Ca(II) and Eu(III) with significant increase in the secondary structure while still maintaining DNA-binding affinity.[42,43] Replacement of a histidine residue for a tryptophan in P3 resulted in an apopeptide with slightly more secondary structure than P3. Binding of Eu(III) and Ce(IV) to this peptide was followed with circular dichroism,[44] and binding of La(III)[45] with tryptophan fluorescence and NMR studies showed formation of a more organized tertiary structure on metal ion binding along with sequence selective nuclease activity.

There has been considerable investigation of the gas phase reactivity of metal ions binding to peptides in order to understand metal influence on secondary protein conformations. In some cases, the oxophilic metal ions bind to the carboxylate group at the C-terminus, thereby capping the helix and allowing favorable interactions between the metal ions and the helix dipole. Most of the research has focused on the energetics of metal binding to the peptides[46−49] and the conformational changes that occur as a result of this

(35) Ghadiri, M. R.; Soares, C.; Choi, C. *J. Am. Chem. Soc.* **1992**, *114*, 825−831.
(36) Ghadiri, M. R.; Case, M. A. *Angew. Chem., Int. Ed. Engl.* **1993**, *32*, 1594−1597.
(37) Ghadiri, M. R.; Soares, C.; Choi, C. *J. Am. Chem. Soc.* **1992**, *114*, 4000−4002.
(38) Case, M. A.; Ghadiri, M. R.; Mutz, M. W.; McLendon, G. L. *Chirality* **1998**, *10*, 35−40.
(39) Zhou, J.; Case, M. A.; Wishart, J. F.; McLendon, G. L. *J. Phys. Chem. B* **1998**, *102*, 9975−9980.
(40) Case, M. A.; McLendon, G. L. *J. Am. Chem. Soc.* **2000**, *122*, 8089−8090.
(41) Gochin, M.; Khorosheva, V.; Case, M. A. *J. Am. Chem. Soc.* **2002**, *124*, 11018−11028.
(42) Kim, Y.; Welch, J. T.; Lindstrom, K. M.; Franklin, S. J. *J. Biol. Inorg. Chem.* **2001**, *6*, 173−181.
(43) Welch, J. T.; Sirish, M.; Lindstrom, K. M.; Franklin, S. J. *Inorg. Chem.* **2001**, *40*, 1982−1984.
(44) Kovacic, R. T.; Welch, J. T.; Franklin, S. J. *J. Am. Chem. Soc.* **2003**, *125*, 6656−6662.
(45) Welch, J. T.; Kearney, W. R.; Franklin, S. J. *Proc. Natl. Acad. Sci. U.S.A.* **2003**, *100*, 3725−3730.
(46) Klassen, J. S.; Anderson, S. G.; Blades, A. T.; Kebarle, P. *J. Phys. Chem.* **1996**, *100*, 14218−14227.

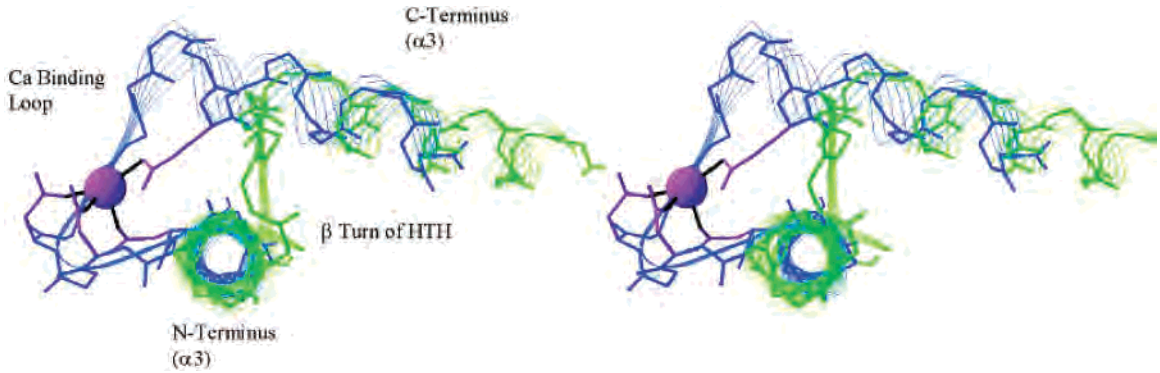

Figure 3. Stereoview of the overlay of engrailed HTH region (α2-α3; 1ENH) and one EF-hand of parvalbumin (5PAL) to illustrate that the helical axes are collinear. Engrailed is shown in green, parvalbumin in blue, and the Ca(II) ions with the ligands in magenta. The figure is taken from Figure 1 of the following reference: Kim, Y.; Welch, J. T.; Lindstrom, K. M.; Franklin, S. J. Chimeric HTH motifs based on EF-hands. *J. Biol. Inorg. Chem.* **2001**, *6*, 175. Copyright 2001, SBIC. Reprinted by permission of Springer.

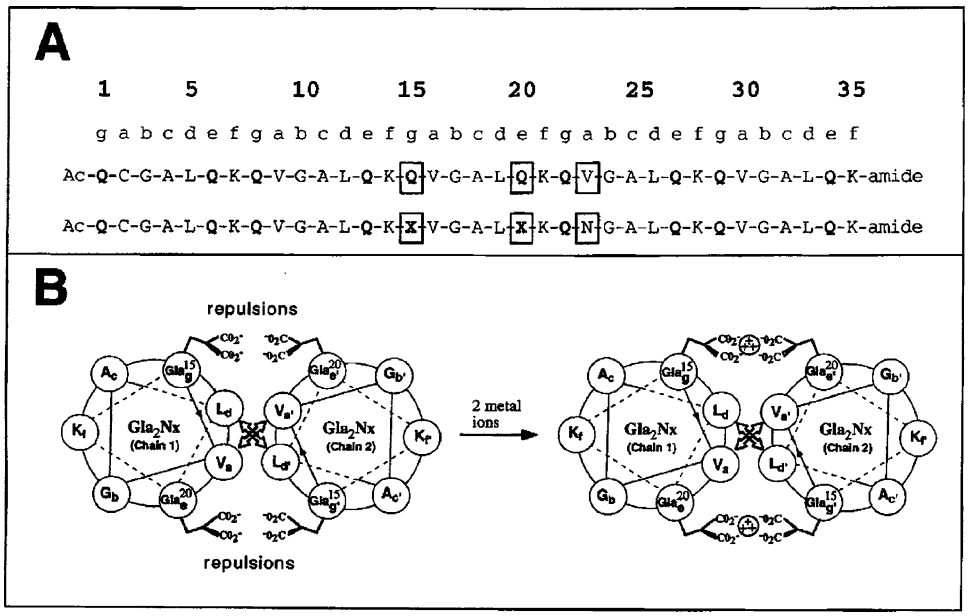

Figure 4. (A) Sequences of the "native" 35-residue model coiled coil peptide (top) and the metal-binding analogue Gla_2Nx (bottom). A Cys residue at position 2 (heptad position a) allows formation of an interchain disulfide bridge. In Gla_2Nx, the Gla residues are represented by X. (B) Cross-sectional helical wheel representation of the middle heptad (residues 15−21) of Gla_2Nx in the absence (left) and presence (right) of bound metal ions. Interchain a−a′ and d−d′ van der Waals packing interactions occur in the hydrophobic core between Val and Leu residues, respectively, and are indicated with arrows. Reprinted with permission from ref 56. Copyright 1998 American Chemical Society.

binding.[50−52] A number of research groups have also investigated the fragmentation of metalated-peptides,[53,54] and it appears that fragment peaks are oftentimes strongly influenced by the conformation of the gas phase protein-ion prior to activation. In general, though fragmentation data may provide information about the transition state of the complex, little is known about the influence of the metal ion on the low-lying states of the metal ion−peptide conformation in the gas phase.

(b) Metal Induced Folding of Random Coils to Generate α-Helical Coiled Coils. In the case of coiled coils, two and three stranded varieties are the most common. Using this motif, a disulfide bridged two stranded α-helical coiled coil peptide containing two identical 35 residue polypeptide chains was designed.[55,56] This peptide was seen to undergo a transition from a random coil to an α-helical conformation upon binding of a metal ion. Cysteine substitution for a valine in the native heptad repeat sequence $Q_gV_aG_bA_cL_dQ_eK_f$ assisted in forming an interhelical disulfide bridge bond. This peptide was used as a good control for studying electrostatic interactions as all the "e" and "g" positions contained Gln residues. The disulfide bridge formation promoted the formation of a parallel coiled coil and simplified the folding mechanism from a bimolecular to a unimolecular one. Two γ-carboxyglutamic acid substitutions for glutamine (Q) residues at positions 15 and 20 generated a new peptide possessing metal ion binding sites as shown in Figure 4. In the absence of any metal ions, the two strands were repelled by electrostatic repulsion between the negatively charged side

(47) Wyttenbach, T.; Bushnell, J. E.; Bowers, M. T. *J. Am. Chem. Soc.* **1998**, *120*, 5098−5103.
(48) Cerda, B. A.; Hoyau, S.; Ohanessian, G.; Wesdimiotis, C. *J. Am. Chem. Soc.* **1998**, *120*, 2437−2448.
(49) Hoyau, S.; Ohanessian, G. *Chem.—Eur. J.* **1998**, *4*, 1561−1569.
(50) Taraszka, J. A.; Li, J.; Clemmer, D. E. *J. Phys. Chem. B* **2000**, *104*, 4545−4551.
(51) Kohtani, M.; Kinnear, B. S.; Jarrold, M. F. *J. Am. Chem. Soc.* **2000**, *122*, 12377−12378.

chains of the γ-carboxyglutamic acids at position 15 on one chain with that at position 20 on the other chain resulting in a random-coil-like secondary structure with a molar ellipticity of only -2500 deg cm^2 dmol^{-1} at 222 nm. However, the folded metal bound peptide formed a stable moiety (molar ellipticity of -34000 deg cm^2 dmol^{-1} with La(III)) showing an α-helical structure. The metal titration monitored indirectly by circular dichroism, and directly by nuclear magnetic resonance spectroscopy, showed the specific binding of two metal ions per two-stranded coiled coil. The metals bound to the two-stranded coiled coil in a cooperative manner. Metal dissociation constants (K_d's) for the first metal binding of 0.6 ± 0.3 μM for La(III), 0.4 ± 0.2 μM for Yb(III), 1.7 ± 0.3 μM for Zn(II), and 18 ± 2 mM for Ca(II) were estimated from the circular dichroism studies.

Using the same heptad repeat motif, Tanaka et al. designed a parallel three stranded coiled coil peptide (IZ) with the amino acid sequence YGG(IEKKIEA)$_4$.[57] Replacement of one or both isoleucine (I) residues on the third heptad with one or two histidine (H) residues generated the peptides (IZ-3adH)[58] and (IZ-3aH)[59] showing random-coil-like secondary structure in aqueous solution. However, in the presence of a transition metal ion, the peptides were induced to assemble into three stranded coiled coils. Fluorescence quenching analysis showed the peptides to be parallel. The binding of transition metals (Co(II), Cu(II), and Zn(II)) was followed by circular dichroism, and dissociation constants of 35 ± 1 μM for Co(II), 17 ± 1 μM for Cu(II), and 23 ± 2 μM for Zn(II) were calculated. Ni(II) showed the highest affinity for binding to the peptide IZ-3adH ($K_d = 5.0 \pm 0.3$ μM). Binding of the paramagnetic Ni(II) ion led to perturbation of the line width showing evidence of broadening. In the absence of the metal ion, the imidazole protons from the His residues appeared at 7.03 and 7.90 ppm. On addition of Ni(II), these peaks gradually broadened until they finally disappeared. This final disappearance occurred on addition of 1 equiv of Ni(II) for three IZ-3adH molecules, indicating that all six of the His residues may be magnetically equivalent and binding to the Ni(II) ion providing an octahedral geometry for the central metal ion (Figure 5). However, Ni(II) did not bind to IZ-3aH. After the report of Dieckmann et al. on TRIL16C binding of Hg(II) as a trigonal complex,[60] Tanaka et al. replaced the isoleucine residues with alanine (A) at the 18th position and cysteine (C) at the 22nd position[61] leading to similar disruption of the nativelike secondary structure. The 18th position in the sequence of the peptide refers to an "*a*" position and 22nd the "*d*" position of the third heptad. Both these residues are directed toward the core of the coiled coil. As expected, these replacements created a soft metal ion binding site where the binding of Cd(II) and Hg(II) was monitored with circular dichroism and ^{113}Cd NMR spectroscopy. These studies showed that metal ions could induce an unstructured form of the peptide to fold into a three stranded coiled coil.

Figure 5. Side view of the tertiary model of the Ni(II) complex of IZ-3adH. The six His side chains are shown by the sticks with the three helix backbones. The Ni(II) is indicated by a sphere. Reprinted with permission from ref 58. Copyright 1998 American Chemical Society.

Many groups have also been interested in incorporating cofactors to create functionally active peptides.[62−65] For example, there are several instances of small peptide motifs or "maquettes" that bind metalloporphyrins for studying artificial heme proteins.[66−69] In one case, the porphyrin is used as an anchor to form a four-helix bundle that forms a

(52) Hu, P.; Gross, M. L. *J. Am. Chem. Soc.* **1993**, *115*, 8821−8828.
(53) Hu, P.; Sorensen, C.; Gross, M. L. *J. Am. Soc. Mass Spectrom.* **1995**, *6*, 1079−1085.
(54) Nemirovskiy, O. V.; Gross, M. L. *J. Am. Soc. Mass Spectrom.* **1998**, *9*, 1285−1292.
(55) Kohn, W. D.; Kay, C. M.; Hodges, R. S. *J. Pept. Res.* **1998**, *51*, 9−18.
(56) Kohn, W. D.; Kay, C. M.; Sykes, B. D.; Hodges, R. S. *J. Am. Chem. Soc.* **1998**, *120*, 1124−1132.
(57) Suzuki, K.; Hiroaki, H.; Kohda, D.; Tanaka, T. *Protein Eng.* **1998**, *11*, 1051−1055.
(58) Suzuki, K.; Hiroaki, H.; Kohda, D.; Nakamura, H.; Tanaka, T. *J. Am. Chem. Soc.* **1998**, *120*, 13008−13015.
(59) Kiyokawa, T.; Kanaori, K.; Tajima, K.; Koike, M.; Mizuno, T.; Oku, J.; Tanaka, T. *J. Pept. Res.* **2004**, *63*, 347−353.
(60) Dieckmann, G. R.; McRorie, D. K.; Tierney, D. L.; Utschig, L. M.; Singer, C. P.; O'Halloran, T. V.; Penner-Hahn, J. E.; DeGrado, W. F.; Pecoraro, V. L. *J. Am. Chem. Soc.* **1997**, *119*, 6195−6196.
(61) Li, X. Q.; Suzuki, K.; Kanaori, K.; Tajima, K.; Kashiwada, A.; Hiroaki, H.; Kohda, D.; Tanaka, T. *Protein Sci.* **2000**, *9*, 1327−1333.
(62) Gibney, B. R.; Dutton, P. L. *Protein Sci.* **1999**, *8*, 1888−1898.
(63) Mutz, M. W.; Case, M. A.; Wishart, J. F.; Ghadiri, M. R.; McLendon, G. L. *J. Am. Chem. Soc.* **1999**, *121*, 858−859.
(64) Benson, D. E.; Wisz, M. S.; Hellinga, H. W. *Proc. Natl. Acad. Sci. U.S.A.* **2000**, *97*, 6292−6297.
(65) Akerfeldt, K. S.; Kim, R. M.; Camac, D.; Groves, J. T.; Lear, J. D.; DeGrado, W. F. *J. Am. Chem. Soc.* **1992**, *114*, 9656−9657.
(66) Gibney, B. R.; Mulholland, S. E.; Rabanal, F.; Dutton, P. L. *Proc. Natl. Acad. Sci. U.S.A.* **1996**, *93*, 15041−15046.
(67) Gibney, B. R.; Rabanal, F.; Skalicky, J. J.; Wand, A. J.; Dutton, P. L. *J. Am. Chem. Soc.* **1997**, *119*, 2323−2324.
(68) Gibney, B. R.; Rabanal, F.; Skalicky, J. J.; Wand, A. J.; Dutton, P. L. *J. Am. Chem. Soc.* **1999**, *121*, 4952−4960.
(69) Lombardi, A.; Nastri, F.; Pavone, V. *Chem. Rev.* **2001**, *101*, 3165−3189.

proton channel through a lipid bilayer.[70] Dutton and Gibney[71,72] have pioneered the incorporation of hemes into soluble 4-helix bundles. Benson et al. have done similar work with peptide-sandwich mesoheme induced folding complexes[73−76] and histidine coordinated helical hemeprotein models.[77−79] In the same vein, Suslick et al. have designed monomeric 15-mer peptides that bind to metalloporphyrins in a 1:2 complex[80] and examined the effect of the sequences of the peptides on their association affinities to the metalloporphyrins, their secondary structures, and electrochemical properties. It was observed that binding of the peptides to metalloporphyrins produced related changes in the secondary structure of the peptides leading to a large increase in the helicity. At the same time, it was noted that noncoordinating hydrophobic residues flanking the central histidine residue binding to the metalloporophyrin contributed as much as 4.5 kcal/mol to the overall stability of the complex and the association constant increased by a factor of 1.6×10^4 as the number of hydrophobic residues were increased.[81] Disulfide bridge incorporation in the peptides produced hairpin and cyclic peptides and increased their binding to heme by 5×10^5 compared to histidine alone.[82] Consistent with earlier work, significant changes in the secondary structure were also observed, and ∼90% helicity was seen for the cyclic peptides in the presence of porphyrin. The work on this family of cyclic peptides was extended to the effect of electrostatic and salt bridge interactions on the 3-dimensional structure showing distinct "nativelike" properties similar to small proteins.[83]

Metal ion-binding domains of naturally occurring proteins have often been incorporated in sequences to create de novo designed artificial peptides mimicking the functional properties of their natural counterparts. Zinc binding domains of prototypical zinc finger peptides,[84−86] calmodulin-like peptides,[87] heavy-metal ion binding proteins,[88] and thermolysin[89] have shown that binding of metal ions to these artificial peptides significantly increases their extent of folding. Oftentimes, the protein stabilizing metal ion is seen to bind at the α-helix terminus and assist in the folding process by supplying secondary structural constraints to the unfolded species.[90,91]

(2) Metal Binding to Folded de Novo Designed Proteins/Peptides and β-Turns and β-Sheets

The ability to design peptidic sequences that fold into predictable structures without the aid of stabilizing factors such as disulfide bonds or metal binding sites and, subsequently, to bind specified ligands and catalyze new reactions is an important goal of de novo design.

(a) Metal Binding to Folded α-Helical Peptides. In addition to metal induced folding of secondary structures of peptides, considerable work has been done on the design of electron transfer sites across the surface of metalloproteins[92−95] and also within the framework of a polypeptide backbone structure leading to the development of coiled coil structures containing mono hemes,[62,96,97] multiple hemes,[98−100] di-iron clusters,[1,101] iron−sulfur clusters,[66,102] copper,[103,104] calcium,[105] and bridging metal assemblies.[106] More recently, attempts have been made to generate sites that mimic the functional

(70) Kim, R. M.; Fate, G. D.; Gonzales, J. E.; Lahiri, J.; Ungashe, S. B.; Groves, J. T. *Self assembly, catalysis and electron transfer with metalloporphyrins in phospholipid membranes*; Kluwer Academic Publishers: Dordrecht, The Netherlands, 1995; Vol. 459.
(71) Gibney, B. R.; Dutton, P. L. *Adv. Inorg. Chem.* **2001**, *51*, 409−455.
(72) Reedy, C. J.; Gibney, B. R. *Chem. Rev.* **2004**, *104*, 617−649.
(73) Arnold, P. A.; Benson, D. R.; Brink, D. J.; Hendrich, M. P.; Jas, G. S.; Kennedy, M. L.; Petasis, D. T.; Wang, M. X. *Inorg. Chem.* **1997**, *36*, 5306−5315.
(74) Benson, D. R.; Hart, B. R.; Zhu, X.; Doughty, M. B. *J. Am. Chem. Soc.* **1995**, *117*, 8502−8510.
(75) Liu, D. H.; Williamson, D. A.; Kennedy, M. L.; Williams, T. D.; Morton, M. M.; Benson, D. R. *J. Am. Chem. Soc.* **1999**, *121*, 11798−11812.
(76) Kennedy, M. L.; Liu, D. H.; Gibney, B. R.; Dutton, P. L.; Benson, D. R. *J. Inorg. Biochem.* **1999**, *74*, 190−190.
(77) Cowley, A. B.; Lukat-Rodgers, G. S.; Rodgers, K. R.; Benson, D. R. *Biochemistry* **2004**, *43*, 1656−1666.
(78) Lee, K. H.; Kennedy, M. L.; Buchalova, M.; Benson, D. R. *Tetrahedron* **2000**, *56*, 9725−9731.
(79) Lee, K. H.; Benson, D. R.; Kuczera, K. *Biochemistry* **2000**, *39*, 13737−13747.
(80) Huffman, D. L.; Rosenblatt, M. M.; Suslick, K. S. *J. Am. Chem. Soc.* **1998**, *120*, 6183.
(81) Huffman, D. L.; Suslick, K. S. *Inorg. Chem.* **2000**, *39*, 5418−5419.
(82) Rosenblatt, M. M.; Huffman, D. L.; Wang, X.; Remmer, H. A.; Suslick, K. S. *J. Am. Chem. Soc.* **2002**, *124*, 12394−12395.
(83) Rosenblatt, M. M.; Wang, J. Y.; Suslick, K. S. *Proc. Natl. Acad. Sci. U.S.A.* **2002**, *100*, 13140−13145.
(84) Merkle, D. L.; Schmidt, M. H.; Berg, J. M. *J. Am. Chem. Soc.* **1990**, *113*, 5450−5451.
(85) Krizek, B. A.; Amann, B. T.; Kilfoil, V. J.; Merkle, D. L.; Berg, J. M. *J. Am. Chem. Soc.* **1991**, *113*, 4518−4523.
(86) Michael, S. F.; Kilfoil, V. J.; Schmidt, M. H.; Amann, B. T.; Berg, J. M. *Proc. Natl. Acad. Sci. U.S.A.* **1992**, *89*, 4796−4800.
(87) Siedlecka, M.; Goch, G.; Ejchart, A.; Stitch, H.; Bierzynski, A. *Proc. Natl. Acad. Sci. U.S.A.* **1999**, *96*, 903−908.
(88) Veglia, G.; Porcelli, F.; DeSilva, T.; Prantner, A.; Opella, S. J. *J. Am. Chem. Soc.* **2000**, *122*, 2389−2390.
(89) Kelso, M. J.; Beyer, R. L.; Hoang, H. N.; Lakdawala, A. S.; Snyder, J. P.; Oliver, W. V.; Robertson, T. A.; Appleton, T. G.; Fairlie, D. P. *J. Am. Chem. Soc.* **2004**, *126*, 4828−4842.
(90) Liu, J.; Dai, J.; Lu, M. *Biochemistry* **2003**, *42*, 5657−5664.
(91) Vandermeulen, G. W. M.; Tziatzios, C.; Schubert, D.; Andres, P. R.; Alexeev, A.; Schubert, U. S.; Klok, H. A. *Aust. J. Chem.* **2004**, *57*, 33−39.
(92) Ogawa, M. Y.; Kozlov, G. V. *J. Am. Chem. Soc.* **1997**, *119*, 8377−8378.
(93) Federova, A.; Chaudhari, A.; Ogawa, M. Y. *J. Am. Chem. Soc.* **2002**, *125*, 357−362.
(94) Kornilova, A. Y.; Wishart, J. F.; Xiao, W.; Lasey, R. C.; Federova, A.; Shin, Y.-K.; Ogawa, M. Y. *J. Am. Chem. Soc.* **2000**, *122*, 7999−8006.
(95) Kornilova, A. Y.; Wishart, J. F.; Ogawa, M. Y. *Biochemistry* **2001**, *40*, 12186−12192.
(96) Choma, C. T.; Lear, J. D.; Nelson, M. J.; Dutton, P. L.; Robertson, D. E.; DeGrado, W. F. *J. Am. Chem. Soc.* **1994**, *116*, 856−865.
(97) Sharp, R. E.; Diers, J. R.; Bocian, D. F.; Dutton, P. L. *J. Am. Chem. Soc.* **1998**, *120*, 7103−7104.
(98) Robertson, D. E.; Farid, R. S.; Moser, C. C.; Urbauer, J. L.; Mulholland, S. E.; Pidikiti, R.; Lear, J. D.; Wand, A. J.; Degrado, W. F.; Dutton, P. L. *Nature* **1994**, *368*, 425−432.
(99) Gibney, B. R.; Isogai, Y.; Rabanal, F.; Reddy, K. S.; Grosset, A. M.; Moser, C. C.; Dutton, P. L. *Biochemistry* **2000**, *39*, 11041−11049.
(100) Reedy, C. J.; Kennedy, M. L.; Gibney, B. R. *Chem. Commun.* **2003**, 570−571.
(101) Maglio, O.; Nasti, F.; Pavone, V.; Lombardi, A.; DeGrado, W. F. *Proc. Natl. Acad. Sci. U.S.A.* **2003**, *100*, 3772−3777.
(102) Mulholland, S. E.; Gibney, B. R.; Rabanal, F.; Dutton, P. L. *Biochemistry* **1999**, *38*, 10442−10448.
(103) Orfei, M.; Alcaro, M. C.; Marcon, G.; Chelli, M.; Giananneschi, M.; Kozlowski, H.; Brasun, J.; Messori, L. *J. Inorg. Biochem.* **2003**, *97*, 299−307.
(104) Schnepf, R.; Horth, P.; Bill, E.; Wieghardt, K.; Hildebrandt, P.; Haehnel, W. *J. Am. Chem. Soc.* **2001**, *123*, 2186−2195.
(105) Procyshyn, R. M.; Reid, R. E. *J. Biol. Chem.* **1994**, *269*, 1641−1647.

and spectroscopic character of more complicated structures and to place second coordination sphere interactions within de novo designed scaffolds to model metal sites in natural proteins more completely. A model of the A-cluster carbon monoxide dehydrogenase, a Ni-X-Fe_4S_4 site that has been hard to stabilize with traditional organic ligands, has been successfully characterized within a designed four-helix bundle.[107,108] In addition, combinatorial libraries of peptides have been synthesized that, based on sequence requirements derived from de novo design studies, fold into coiled coils and helical bundles.[109,110]

(b) Metal Binding to *β*-Turns and *β*-Sheets. The area of de novo metalloprotein design has been dominated by the α-helical coiled coil structure. Though a considerable amount of effort has focused on designing *β*-sheetlike secondary structures to probe fundamental insight into the factors affecting protein structure and stability, generally, preparation of chemical models of *β*-sheet is difficult due to the varied complexity of their folding and their propensity for self-association. Therefore, a number of related molecular scaffolds have been used to mimic *β*-sheetlike structure of attached peptide chains and serve as substitute for the *β*-turn in the chemical models of protein secondary structures. Among these are the $\beta_2\alpha$ motif mentioned above for zinc binding peptides,[111−113] α- and *γ*-turns,[114] *β*-hairpin motif peptides,[24,82] and *β*-sheetlike structures.[115−117]

A Specific Example of de Novo Design and Metallopeptide Folding. Through much of the past decade, our group characterized the TRI series of peptides. The parent peptide, TRI, with the amino acid sequence Ac-G(LKALEEK)$_4$G-NH_2 was shown by circular dichroism spectroscopy to form α-helical coiled coils that were very stable to guanidinium denaturation titrations.[118] It was demonstrated that the aggregation state of the coils was sensitive to pH. Below pH 5, where denaturation experiments indicated the peptide was most stable, a 2-stranded coiled coil was the dominant structure. Above pH 6, when all of the glutamate carboxylates were deprotonated, the peptides primarily formed 3-stranded coiled coils. Replacement of a hydrophobic leucine residue with a cysteine in the sequence generated a soft-metal binding site capable of binding heavy metals such as Hg(II),[60] Cd(II),[119] Pb(II),[120] and As(III).[121]

Table 1. Sequences of Peptides Examined in This Study

peptide	sequence
BabyTRI	Ac-G LKALEEK LKALEEK LKALEEK G-NH_2
BabyL9C	Ac-G LKALEEK **C**KALEEK LKALEEK G-NH_2
BabyL12C	Ac-G LKALEEK LKA**C**EEK LKALEEK G-NH_2
TRIL9C	Ac-G LKALEEK **C**KALEEK LKALEEK LKALEEK G-NH_2
TRL12C	Ac-G LKALEEK LKA**C**EEK LKALEEK LKALEEK G-NH_2
GrandL9C	Ac-G LKALEEK **C**KALEEK LKALEEK LKALEEK LKALEEK G-NH_2

Almost exclusively, all of these metals formed trigonal thiolato coordination geometry. To understand the factors involved in the stabilization of trigonal thiolato Hg(II) within the interior of 3-stranded coiled coils, a expansive study was carried out to derive a thermodynamic model for Hg(II) encapsulation.[122] A series of peptides was used in this study to ensure that the derived model was consistent for peptides with differing coiled coil formation constants (K_f). These peptides differed in length and, therefore, in the number of hydrophobic contacts when forming the coiled coil and consequently in their self-association (K_f). The shortest peptides, BabyTRI and BabyL9C (see Table 1), not only gave the smallest formation constant, but also showed less than 20% helicity at 10 *μ*M concentrations in the absence of denaturant, indicating a weakly associated or unassociated coiled coil structure. Interestingly, Baby L9C was shown to stabilize trigonal thiolato Hg(II) within the interior of a 3-stranded coiled coil as observed by the characteristic ligand-to-metal charge-transfer bands in the ultraviolet spectrum.[123] This result challenged the prior notion that a preorganized site is necessary to stabilize alternative coordination geometries around metals in designed peptide systems. The derived thermodynamic model explained how small peptides, unstructured prior to addition of metal, could ultimately stabilize a Hg(II)$(SR)_3^-$ site. This involved the nucleation of a 2-stranded coiled coil by coordination of the Hg(II) to two thiolate ligands, a process that is highly favored for simple thiolate ligands.[124,125] However, at high pH and in the presence of 3 equiv or more of peptide, a trigonal Hg(II)−S_3 structure in a 3-stranded coiled coil was realized. These studies demonstrated that the metalloprotein product resembled neither the modified peptide preference (unfolded)

(106) Costanzo, L. D.; Wade, H.; Geremia, S.; Randaccio, L.; Pavone, V.; DeGrado, W. F.; Lombardi, A. *J. Am. Chem. Soc.* **2001**, *123*, 12749−12757.
(107) Laplaza, C. E.; Holm, R. H. *J. Am. Chem. Soc.* **2001**, *123*, 10255−10264.
(108) Musgrave, K. B.; Laplaza, C. E.; Holm, R. H.; Hedman, B.; Hodgson, K. O. *J. Am. Chem. Soc.* **2002**, *124*, 3083−3092.
(109) Moffet, D. A.; Case, M. A.; House, J. C.; Vogel, K.; Williams, R. D.; Spiro, T. G.; McLendon, G. L.; Hecht, M. H. *J. Am. Chem. Soc.* **2001**, *123*, 2109−2115.
(110) Moffet, D. A.; Certain, L. K.; Smith, A. J.; Kessel, A. J.; Beckwith, K. A.; Hecht, M. H. *J. Am. Chem. Soc.* **2000**, *122*, 7612−7613.
(111) Krizek, B. A.; Merkle, D. L.; Berg, J. M. *Inorg. Chem.* **1993**, *32*, 937−940.
(112) Struthers, M. D.; Cheng, R. P.; Imperiali, B. *Science* **1996**, *271*, 342−345.
(113) Struthers, M. D.; Cheng, R. P.; Imperiali, B. *J. Am. Chem. Soc.* **1996**, *118*, 3073−3081.
(114) Bonomo, R. P.; Casella, L.; Gioia, L. D.; Molinari, H.; Impellizzeri, G.; Jordan, T.; Pappalardo, G.; Rizzarelli, E. *J Chem. Soc., Dalton Trans.* **1997**, 2387−2389.
(115) Venkatraman, J.; Naganagowda, G. A.; Sudha, R.; Balaram, P. *Chem. Commun.* **2001**, 2660−2661.
(116) Schneider, J. P.; Kelly, J. W. *J. Am. Chem. Soc.* **1995**, *117*, 2533−2546.
(117) Platt, G.; Chung, C.; Searle, M. *Chem. Commun.* **2001**, 1162−1163.
(118) Dieckmann, G. R.; McRorie, D. K.; Lear, J. D.; Sharp, K. A.; DeGrado, W. F.; Pecoraro, V. L. *J. Mol. Biol.* **1998**, *280*, 897−912.
(119) Matzapetakis, M.; Farrer, B. T.; Weng, T.-C.; Hemmingsen, L.; Penner-Hahn, J. E.; Pecoraro, V. L. *J. Am. Chem. Soc.* **2002**, *124*, 8042−8054.
(120) Matzapetakis, M.; Pecoraro, V. L. Manuscript in preparation.
(121) Farrer, B.; McClure, C.; Penner-Hahn, J. E.; Pecoraro, V. L. *Inorg. Chem.* **2000**, *39*, 5422−5423.
(122) Farrer, B. T.; Harris, N. P.; Balchus, K. E.; Pecoraro, V. L. *Biochemistry* **2001**, *40*, 14696−14705.
(123) Wright, J. G.; Natan, M. J.; MacDonnell, F. M.; Ralston, D. M.; O'Halloran, T. V. *Prog. Inorg. Chem.* **1990**, *38*, 323−412.
(124) Outten, C.; Outten, F. W.; O'Halloran, T. V. *J. Biol. Chem.* **1999**, *274*, 37517−37524.
(125) Helmann, J. D.; Ballard, B. T.; Walsh, C. T. *Science* **1990**, *247*, 946−948.

nor the metal coordination preference (linear, 2-coordinate), but rather it adopted the designed, well-folded 3-stranded coiled coil with 3-coordinate Hg(II). The folding process is initiated by strong metal complexation to the thiolates; however, peptide−peptide interactions then overwhelm coordination preference to affect the final structure.

Both detailed thermodynamic and kinetic studies have examined the BabyL9C plus Hg(II) system. It was found that Hg(II) reacted in a very fast step to form $Hg(BabyL9C)_2$. The rate-limiting association was formation of $Hg(II)(BabyL9C)_2(H-BabyL9C)$, which, depending on pH, underwent a rapid conversion to $Hg(II)(BabyL9C)_3^-$. This series of steps was called the "stepwise aggregation−deprotonation model" or StepAD model. This system was complicated by an unproductive antiparallel $Hg(II)(BabyL9C)_2(H-BabyL9C)$ species which required a slow kinetic phase for rearrangement to the parallel $Hg(BabyL9C)_3^-$ product.

While the mechanistic understanding of this metal ion induced protein folding process is set at a high level, there are two interesting factors that have not yet been addressed. The first is the observation that the apparent pK_a for the conversion of $Hg(II)(pep)_2(H\text{-}pep)$ to $Hg(II)(pep)_3^-$ is dependent on the location of the cysteine in the peptide sequence. This pK_a is 7.6 for TRIL9C which has cysteine in the "*a*" position and 8.4 for TRIL12C with cysteine in a "*d*" position. These pK_a perturbations are independent of peptide length as identical acidities are found for BabyL9C, TRIL9C, and GrandL9C. Thus, it is possible that the rate of metal induced folding for BabyL9C and BabyL12C could be different. The second observation is that the affinity of BabyL12C to form $(HBabyL12C)_3$ in the absence of a metal is much lower than that of $(HBabyL9C)_3$ because introduction of a cysteine in the "*d*" position is more destabilizing to bundle formation than in an "*a*" position. Furthermore, TRIL9C, TRIL12C, and GrandL9C have sufficiently high affinities to ensure that, at micromolar concentrations, these peptides are found exclusively as $(Hpep)_3$ without unfolded states. These observations taken together suggest that the rate of $Hg(II)(pep)_3^-$ formation may differ between BabyL9C and BabyL12C and that mechanism of metal insertion into TRIL9C and other stable peptides may differ from that elaborated for BabyL9C. New results to address these points will be discussed in this article.

(1) Comparison of Metal Induced Folding between BabyL9C and BabyL12C

(a) Concentration Dependence of Coiled-Coil Association. The coiled coil association constants for each of the two smaller peptides BabyL9C and BabyL12C were determined by titration of increasing concentrations of the peptides into a solution containing 0 μM peptide and monitoring the α-helical signature in the UV CD spectrum. The titration data were evaluated using the association equilibrium for a 3-stranded coiled coil defined by the equilibrium constant K_{assoc}.

$$3(\text{BabyL XC}) \leftrightarrows (\text{BabyL XC})_3 \quad \text{where X} = 9,12 \qquad (1)$$

We know that a peptide within a coiled coil has a greater α-helical character than a peptide that is not associated,

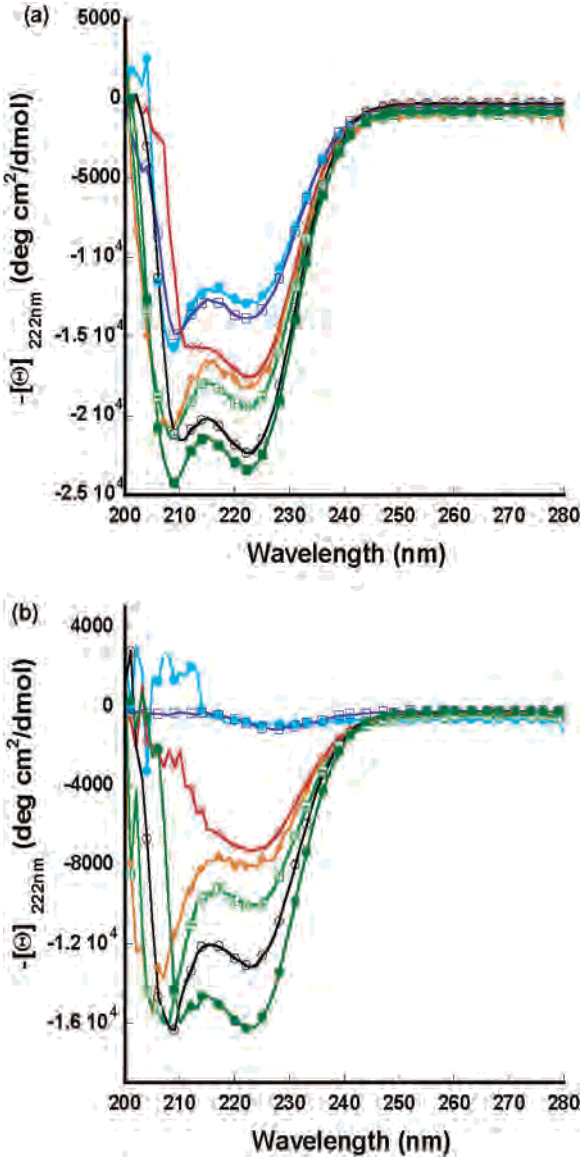

Figure 6. Concentration dependent CD spectra of BabyL9C (A) and BabyL12C (B). Concentrations are 20 μM (●, light blue), 40 μM (□, dark blue), 50 μM (◇, red), 80 μM (◆, orange), 160 μM (□ with +, light green), 320 μM (○, black), and 640 μM (■, dark green).

giving rise to a greater increase in the CD minima signal at 222 nm. For both the peptides, the titration showed an increase in the molar absorptivity of the solutions with increase in peptide concentration consistent with the model in eq 1.

Figure 6 shows the concentration dependent circular dichroism spectra for each of the peptides in the absence of a metal ion. In the case of BabyL9C, the apo-peptide displays spectra characteristic of marginally stable α-helices at low concentrations: a minimum at 208 nm due to α-helix ($\pi-\pi^*$ parallel) contribution and a minimum at 222 nm due to α-helix ($n-\pi^*$) contribution.[126−128] These minima become

(126) Chen, Y. H.; Yang, J. T.; Chau, K. H. *Biochemistry* **1974**, *13*, 3350−3359.
(127) Shoemaker, K. R.; Kim, P. S.; York, E. J.; Stewart, J. M.; Baldwin, R. L. *Nature* **1987**, *326*, 563−567.
(128) Marqusee, S.; Baldwin, R. L. *Proc. Natl. Acad. Sci. U.S.A.* **1987**, *84*, 8898−8902.

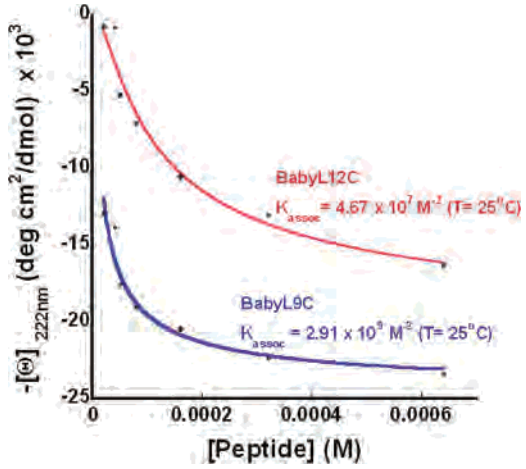

Figure 7. Fits to the concentration dependent titrations of BabyL9C and BabyL12C monitored at 222 nm. Fitting assumes the equilibrium model 3BabyLnC ⇄ (BabyLnC)$_3$ where n = 9, 12.

more pronounced at higher concentrations of peptide showing stronger affinity of the helices for each other. This leads to more pronounced hydrophobic interactions which in turn play a significant role in the overall conformational stability of the peptide. At higher concentrations, the ratio of $\theta_{222}/\theta_{208}$ is slightly lower than 1 indicating a partially unfolded coiled coil structure[129] that is slightly frayed. In case of BabyL12C, however, the structural characterization is more complex. At lower concentrations (up to 40 μM), the spectra are indicative of a random-coil-like conformation. At higher concentrations (80−640 μM), there appear distinct minima at 205 nm [mixture of 2 bands: α-helix ($\pi-\pi^*$ parallel) transition at 208 nm and random coil ($\pi-\pi^*$) transition at 200 nm] and 222 nm [α-helix (n−π^*) transition]. Also, as the concentration increases from 80 to 640 μM, there is a distinct shift in the minimum at 205 nm toward 208 nm indicating more stable α-helical conformation. In the intermediate concentration (50 μM), the spectra are neither consistent with an α-helical nor random-coil-like structure suggesting that an alternate folding pattern may be populated.

While BabyL9C showed an association constant of ∼3 × 10^9 M^{-2} (ΔG = −13.1 kcal/mol) at pH 8.5 at room temperature (Figure 7), BabyL12C is considerably less stable with a lower associative affinity of ∼4.6 × 10^7 M^{-2} (ΔG = −10.4 kcal/mol) consistent with the theory of peptides with cysteine substitution in the "*d*" position being considerably less stable than those in the "*a*" position. Also, while BabyL9C shows an α-helical content of about 66% at the highest concentration ($[\Theta]_{222}$ value of −35000 deg cm^2/dmol is the value expected for a fully helical peptide), BabyL12C is only ∼46% helical at the same concentration.

(b) Relative Affinity of the Peptides for Hg(II). Hg(II)(pep)$_3^-$ displays a characteristic lower energy LMCT at 247 nm easily distinguishable from the higher energy absorption of Hg(II)(pep)$_2$. However, both the peptides differed in their relative affinities for binding to Hg(II) as is evident from Figure 8. While the charge-transfer complex formed between Hg(II) and BabyL9C has an extinction

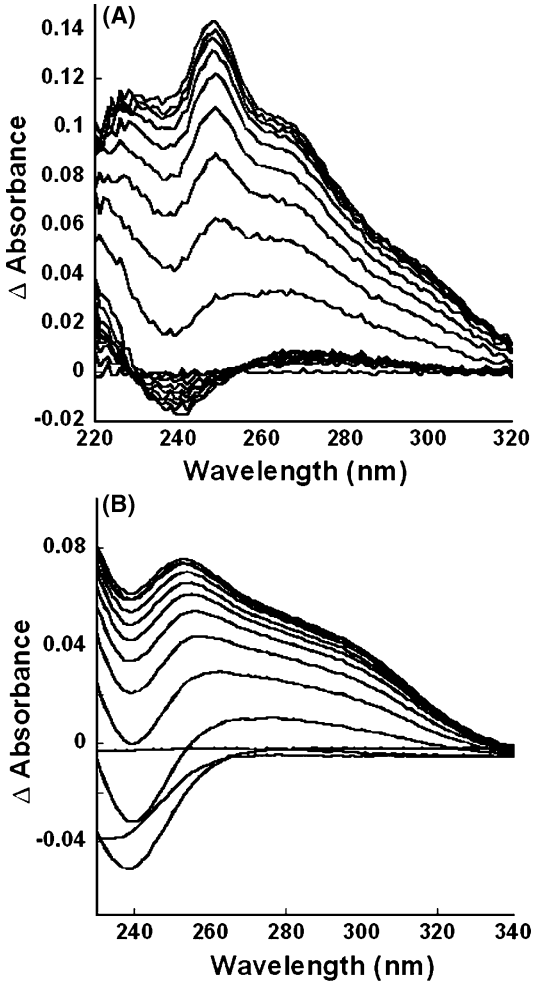

Figure 8. Difference spectra of titrations of solutions of BabyL9C (A) and BabyL12C (B) into a solution containing 10 μM $HgCl_2$ in 50 mM buffer.

coefficient of about 14000 mol^{-1} L cm^{-1}, that between Hg(II) and BabyL12C shows a relatively smaller extinction coefficient of about 8000 mol^{-1} L cm^{-1}, thus showing that although their behavior toward Hg(II) is similar, they are not identical. Thus, Hg(II) nucleates the fold in both the peptides and attains a trigonal geometry, yet it forms a much less well-defined coiled coil in case of BabyL12C.

The binding constant for binding of the third thiolate to Hg(II)(SR)$_2$ was determined in each case using MAPLE 7 and Kaleidagraph 3.0 (by Synergy Software) using the model

$$Hg(II)(SR)_2 + SR^- \leftrightarrows Hg(II)(SR)_3^- \qquad (2)$$

Similar to the association of the peptides in the absence of a metal, in this case as well, the binding constant for BabyL9C with Hg(II) ($1.9 \times 10^5 \pm 389.6$) is greater than that of BabyL12C with Hg(II) ($5 \times 10^4 \pm 168.4$) which can be attributed to the difficulty in the formation of a trigonal bond with Hg(II) in the case of an unfavorable cysteine conformation found in the "*d*" substituted peptides and the inherent lower affinity for forming a 3-stranded coiled coil.

Insilico-mutation followed by partial energy minimization of a similar peptide $CoilV_aL_d$, possessing a similar three stranded coiled coil structure, with cysteine substitution for leucine residues in the hydrophobic core of the peptide shows

(129) Cooper, T. M.; Woody, R. W. *Biopolymers* **1990**, *30*, 657−676.

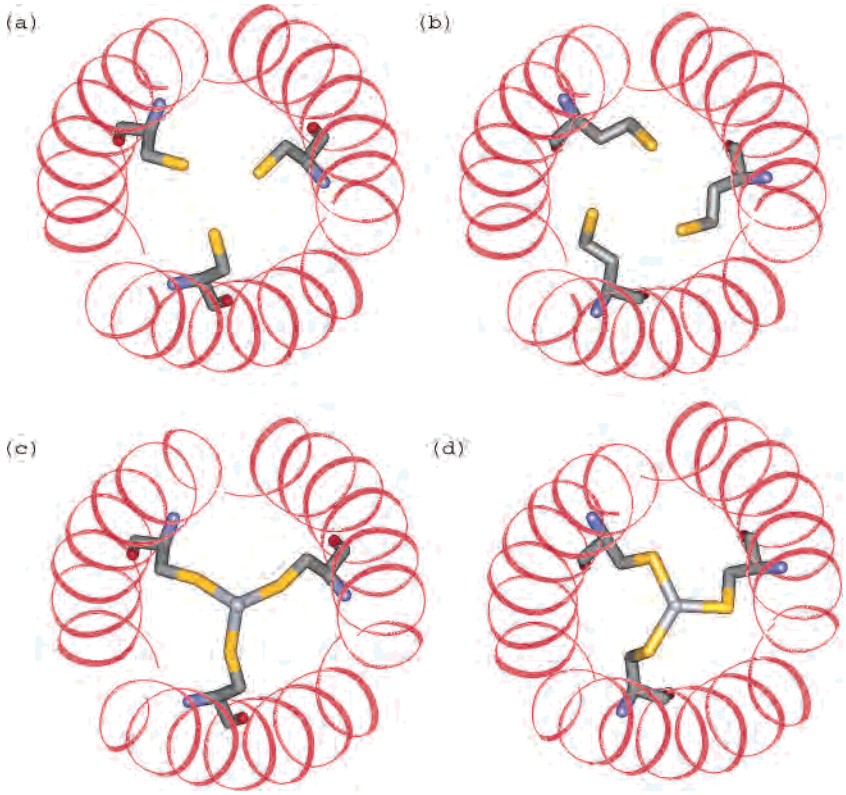

Figure 9. Insilico-mutated models of a similar peptide showing orientations of the residues. (a) Model showing orientation of cysteine residue at 9 ("a" position). (b) Model showing orientation of cysteine residue at 12 ("d" position). (c) Model showing orientation of cysteine in the "a" peptide bound to Hg(II). (d) Model showing orientation of cysteine in the "d" peptide bound to Hg(II).

distinct differences in the orientation of residues placed at the "*a*" position compared with the "*d*" position. The side-chain torsion angles (C−C_α-C_β−SH) (χ_1) for the apo-peptides are 164° for the "*a*" substituted peptide and 158.5° for the "*d*" substituted peptide (Figure 9). In this mode, the C_β-SH bond of the "*a*" substituted peptide is oriented more directly toward the central metal binding core of the peptide, thereby displaying a more favorable orientation for metal binding than its "*d*" counterpart. This is observed on modeling the same peptide in the presence of a Hg(II) ion. It is seen that, on placing a Hg(II) ion in the middle of the hydrophobic core of the peptide, the "*a*" substituted peptide binds to the metal without any change in the (C−C_α-C_β−SH) (χ_1) torsion angle. The "*d*" peptide, on the other hand, has to twist itself from its normal position and orient more toward the center of the core to bind the metal. In doing so, the (C−C_α−C_β−SH) (χ_1) torsion angle now becomes −76.9°, thereby having to twist unfavorably by 235.4° from its unmetalated position. This justifies the favorable and more stronger binding affinity of the "*a*" peptide for Hg(II).

(c) Temperature Dependence of Affinity of the Peptides for Hg(II). Temperature is seen to affect distinctly the overall binding affinity of the peptides toward Hg(II); however, the effect is seen to be opposite for the two peptides. As the temperature rises, the binding affinity of Hg(II) with the peptide BabyL9C is seen to increase. In contrast, the binding becomes weaker at elevated temperature for BabyL12C. This opposite effect can be explained by considering the nature of self-association of the peptides in the absence of a metal ion as shown above. Though both peptides are not completely folded at the micromolar concentrations (80−100 μM) at which these titrations are conducted, BabyL9C still folds to a partial degree as an α-helical coiled coil and hence is associated in a small percentage as a 2- or 3-stranded coiled coil. BabyL12C has multiple folded states and seems to populate an alternate folding pattern, some of which may correspond to structural forms of unassociated peptides. With the rise in temperature, there is expected to be some extent of N and C terminus fraying for BabyL9C, an observation that has been supported by 2D NMR experiments. It is expected that $(HBabyL9C)_3$ would be more unstable due to fraying than $Hg(II)(BabyL9C)_2$ or $Hg(II)(BabyL9C)_3^-$ because the unmetalated aggregate is not tethered together by the Hg(II). Thus, recognizing $(HBabyL9C)_3$ should dissociate to HBabyL9C more easily at higher temperature and that free HBabyL9C should strongly react with $Hg(II)(BabyL9C)_2$ to give $Hg(II)(BabyL9C)_3^-$, it is expected that the reaction of $Hg(II)(BabyL9C)_2$ with $(HBabyL9C)_3$ should also be driven toward the product $Hg(II)(BabyL9C)_3^-$. In contrast, BabyL12C displays a very different secondary conformation that likely is related to the monomeric form of the peptide. If this alternate secondary structure was less stable than the α-helix as a function of temperature, the effect of temperature increase would cause the newly formed α-helices to associate in the unmetalated state which would hinder the formation of $Hg(II)(BabyL12C)_3^-$. For both the peptides, plots of ln(K) versus $1/T$ indicate that the $\Delta G°$ of complex formation is governed by a $\Delta H°$ of 19(2) kcal/mol for BabyL9C and −3(9) kcal/mol for BabyL12C and a $\Delta S°$ of 90(5) cal/mol K for BabyL9C and 10(1) cal/mol K for BabyL12C. These

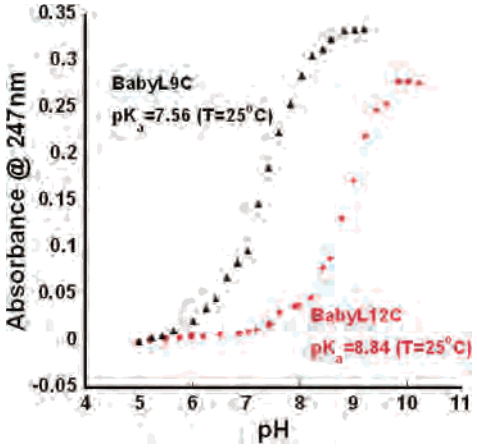

Figure 10. pH titrations of Hg complexes of BabyL9C (▲) and BabyL12C (●) monitored at 247 nm.

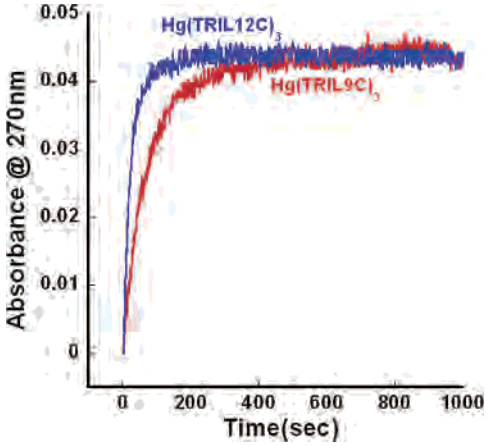

Figure 11. Kinetic traces of Hg(II) binding to TRIL9C and TRIL12C monitored by stopped-flow experiments by mixing 10 μM $HgCl_2$ and 100 μM peptide in 50 mM buffer containing 100 mM KCl at 270 nm (10 °C).

thermodynamic parameters are consistent with a negative free energy change for complex formation that is greater in magnitude for BabyL9C compared to BabyL12C.

(d) pK_a's of the Mercurated Complexes. Initial studies of Hg(II) binding by TRI L12C suggested that this "*d*" substituted peptide would not bind Hg(II) in a trigonal geometry. Investigation of this system more fully has made us realize that the differential behavior lay in the pK_a of the Hg(II) complexes. The pK_a refers to the deprotonation of the third thiol from the folded 3-stranded moiety encapsulating a linear Hg(II). It is important to note that the apparent pK_a value for the longer "*a*" peptide was ~7.6 while that of the "*d*" peptide was ~8.4. Following these observations, pH titrations were performed on the smaller Baby peptides to see if the unfolded nature of these weakly associated peptides had any significant role on this deprotonation step.

Figure 10 shows pH titrations of the mercury solutions of BabyL9C and BabyL12C. The peptide having cysteine in the "*a*" position (BabyL9C) shows an apparent pK_a of 7.6 ± 0.2 while the "*d*" substituted peptide (BabyL12C) shows a pK_a of 8.4 ± 0.2, which is similar to what was seen for the longer TRI peptides. Thus, the effect of decreased self-affinity of the Baby peptides does not seem to affect the final step of complex formation. Clearly, the pK_a perturbations are dependent on the final folded state of the $Hg(II)(pep)_3^-$ system and the orientation of the coordinating thiolate residues, but as predicted from the StepAD model, they do not influence nucleation of the peptide fold.

(e) Kinetics of Metal Binding to the Peptides. The thermodynamic results were used to propose a kinetic mechanism for folding of an unstructured peptide like BabyL9C around a trigonal thiolato Hg(II)[130] that has been termed the StepAD mechanism. Corresponding to the differences in thermodynamic parameters between BabyL9C and BabyL12C, we wanted to examine whether one would observe a kinetic difference in rate for "*a*" versus "*d*" substituted peptides. We observe that the half-life of the reaction between BabyL9C and Hg(II) is about 200 ms while that for BabyL12C with Hg(II) is less than 4 ms. The latter rate is faster than the mixing time of the stopped flow spectrophotometer precluding a more precise rate determination. We suggest that the origin of this enhanced rate is due primarily to the much weaker self-association preference of BabyL12C. The StepAD mechanism requires metal to bind from an unassociated and unfolded state. Because there is a greater concentration of BabyL12C in solution as monomers than is present for BabyL9C, the presence of Hg(II) more rapidly nucleates BabyL12C to $Hg(II)(pep)_2$ which immediately converts to $Hg(II)(pep)_3^-$.

The results discussed above clearly show that adjustment in the position of the thiol from an "*a*" position in the case of BabyL9C to a "*d*" position for BabyL12C has resulted in a peptide with lower self-association affinity, weaker binding with Hg(II), and a considerably faster kinetic profile for metal ion insertion. Despite the observed differences, it can be expected that the folding pathway for metal ion insertion by BabyL12C would be similar to the StepAD mechanism as the initial state of the peptide is still an unassociated monomer, the reaction of $Hg(BabyL12C)_2$ plus Hg(HBabyL12C) to form $Hg(BabyL12C)_3^-$ is still very fast, and the acidity of the final deprotonation is invariant from other "*d*" substituted peptides.

An underlying assumption in the previous discussion is that metal insertion into a prefolded 3-stranded coiled coil will be slower than that in the unfolded peptides. The longer TRI peptides which are fully folded under our experimental conditions and which have higher Hg(II) affinities will allow us to test this hypothesis.

(2) Comparison of Metal Ion Insertion between Unfolded BabyL9C/BabyL12C and Folded TRIL9C/TRIL12C/GrandL9C Peptides

Unlike their smaller counterparts, TRI and Grand peptides are significantly folded at the micromolar concentrations at which most of our experiments were performed. Given that the StepAD mechanism was derived for unfolded peptides, it might be expected that metal insertion into a prefolded peptide would show different mechanistic features and would most likely follow a different pathway. Two limiting processes (Figure 12) are termed the "breathing mechanism"

(130) Farrer, B.; Pecoraro, V. L. *Proc. Natl. Acad. Sci. U.S.A.* **2003**, *100*, 3760−3765.

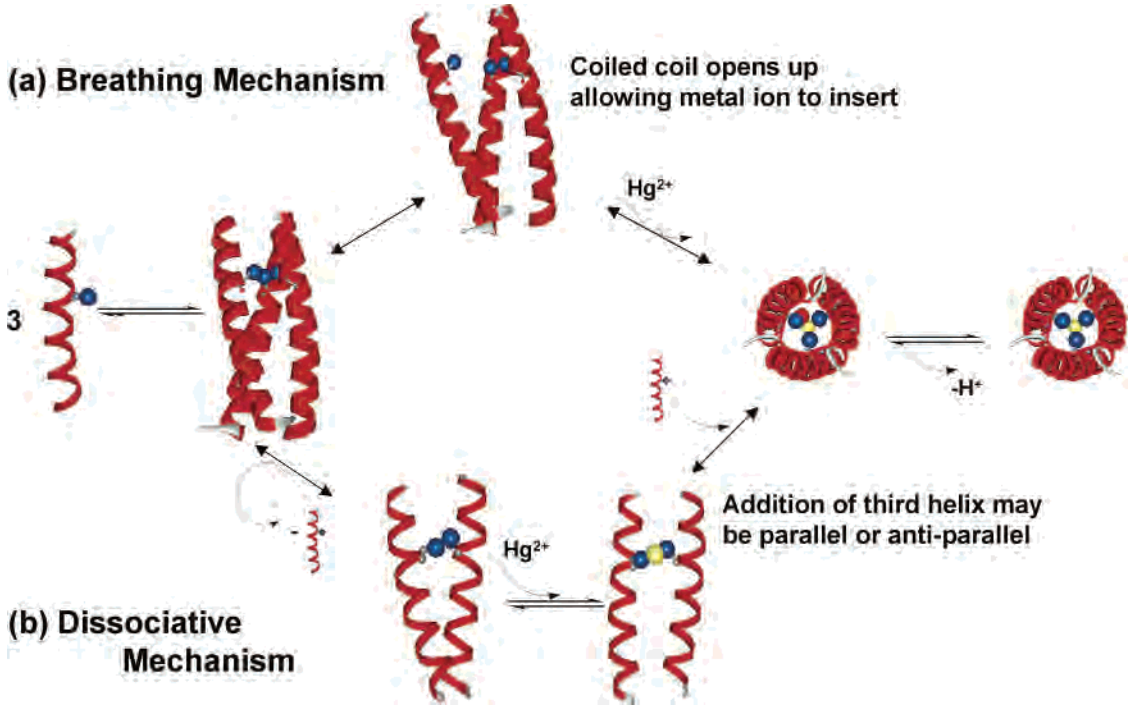

Figure 12. Possible mechanisms for insertion of Hg(II) into the folded peptides.

and the "dissociation mechanism". While we are unable to mechanistically distinguish these processes at this time, we will herein present data that addresses the general rates of metal ion binding to prefolded de novo designed peptides.

(a) Temperature-Dependent pH Titrations of the Peptides. Temperature is seen to play an important role in the conversion of Hg(II)$(pep)_2(Hpep)$ to Hg(II)$(pep)_3^-$. However, as was the case for the temperature-dependent binding affinities seen before for the unassociated Baby peptides, temperature is seen to affect the longer "*a*" substituted peptide differently from the "*d*" peptide. With the rise in temperature, the pK_a's for TRIL9C increase while those for TRIL12C decrease. Thus, although the pK_a perturbations occur in the folded state, Hg(II)$(pep)_2(Hpep)$, and are not a determining factor in protein folding, the position and orientation of the cysteine residues is again seen to play a significant role in the actual Hg(II)$(pep)_3^-$ product formation. A plot of ln K_a versus $1/T$ for the peptide TRIL9C shows that the free energy for complex formation for TRIL9C exhibits a $\Delta H°$ of $-3(4)$ kcal/mol and a $\Delta S°$ of $-45(5)$ cal/mol K. Given the error in determination of the enthalpy, this value is within the range normally associated with binding a third thiolate to a linear, bis(thiolate)Hg(II) complex ($\sim$1.2 kcal/mol).[131]

In case of the "*d*" substituted peptide, TRIL12C, the $\Delta G°$ of complex formation is governed by a $\Delta H°$ of 3(1) kcal/mol and a $\Delta S°$ of $-22(2)$ cal/mol K leading to a lower negative free energy value compared to TRIL9C. The positive enthalpy suggests that there is an enthalpic barrier to the formation of the third thiolate bond in the final trigonal complex. To verify whether such an effect is seen for the smaller unassociated peptides, temperature-dependent pH titrations were conducted with BabyL12C. Similar to what was seen before, the pK_a's for BabyL12C also fall with the rise in temperature. A plot of ln K_a versus $1/T$ for the titrations for BabyL12C determines an $\Delta H°$ of 5(5) kcal/mol and a $\Delta S°$ of $-21(1)$ cal/mol K. These experiments again reiterate the point that metal ion complexation behaviors in "*a*" versus "*d*" sites are significantly different.

(b) Kinetics of Metal Binding to the Peptides. As was suggested above, it is unlikely that the mechanism of metal ion insertion into the longer TRI and Grand peptides will be analogous with the mechanism proposed for an unassociated coiled coil. Preliminary results from the encapsulation of Hg(II) by the more structured TRIL9C, TRIL12C, and GrandL9C show a much different reaction profile than that observed for BabyL9C and BabyL12C. The most striking difference is the well-separated biphasic behavior of Hg(II) encapsulation by these peptides. The two phases of the reaction are most easily rationalized by the dissociation mechanism. If metal insertion requires the loss of a peptide from the three-stranded coiled coil, then the initial reformation of a parallel 3-stranded coiled coil with bound Hg(II) giving the 3-stranded coiled coil would be seen as a fast phase. If the replaced peptide reassociated with the coiled coil to give an antiparallel 3-stranded coiled coil, a spectroscopically invariant digonal Hg(II) complex would result. Due to the stability of the aggregate, TRIL9C should form a more stable misfolded state than BabyL9C. Therefore, the dissociation of the misfolded state to allow for the proper formation of the spectroscopically observable parallel 3-stranded coiled coil with trigonal Hg(II) would be slower than that for BabyL9C, yielding a slower second phase. This result is observed.

However, even in the cases of the more structured TRI and Grand peptides, we do observe a similar pattern as seen

(131) Utschig, L. M.; Wright, J. G.; O'Halloran, T. V. *Biochemical and spectroscopic probes of Hg(II) coordination environments in protein*; Academic Press Inc.: San Diego, CA, 1993; Vol. 226.

Table 2. Thermodynamic and Kinetic Parameters for Metal Insertion into the Peptides

	temperature-dependent binding of Hg			temperature-dependent pH titrations		
peptide	$\Delta H°$ (kcal/mol)	$\Delta S°$ (cal/mol K)	pK_a	$\Delta H°$ (kcal/mol)	$\Delta S°$ (cal/mol K)	half-life (s)
BabyL9C	−19(2)	90(5)	7.6 ± 0.2			0.2
BabyL12C	−3(9)	10(1)	8.4 ± 0.2	5(5)	−21(1)	0.002
TRIL9C			7.7 ± 0.2	−3(4)	−45(5)	42.5
TRIL12C			8.4 ± 0.2	3(1)	−22(2)	15.8
GrandL9C			7.6 ± 0.2			1576

before with the smaller Baby peptides. The "*d*" substituted peptide, TRIL12C, like its smaller counterpart is seen to show a faster reaction profile as compared to the "*a*" substituted peptide, TRIL9C, as shown in Figure 11. In fact, the half-life of the reaction between $HgCl_2$ and TRIL12C which is about 15.8 s is almost three times faster then that for TRIL9C with $HgCl_2$ (42.5 s), see Table 2. This observation is consistent with either the breathing or dissociation mechanisms since the TRIL12C peptide has lower self-affinity than TRIL9C. In the case of the reaction between $HgCl_2$ and the longest peptide GrandL9C, the half-life is about 1576 s, showing that, as the length (and consequently the self-association affinity) of the peptide increases, the rate of metal ion insertion becomes considerably slower.

So what could be a possible mechanism of metal binding in the case of these associated peptides? Obviously for these longer peptides, the StepAD mechanism would be inappropriate unless a 3-stranded coiled coil fully dissociated to monomers prior to metal binding. The two limiting mechanisms mentioned earlier are presented in Figure 11. The first mechanism is one that we have termed the "breathing mechanism". In this mechanism, the first step is slow and at least partially rate-determining in which the 3-stranded coiled coil opens up slightly to allow for the insertion of the metal ion to form $Hg(II)(pep)_2(Hpep)$. The final step would be a fast loss of the proton to form the trigonal Hg(II) complex. An appreciable concentration of the misfolded, antiparallel form is not anticipated via this mechanism because ^{1}H NMR experiments have demonstrated that the unmetalated peptides are greater than 90% parallel. The second mechanism termed the "dissociation mechanism" requires a dissociation of a peptide from the 3-stranded coiled coil giving the less stable 2-stranded form. This more open coiled coil could then undergo Hg insertion to form the $Hg(pep)_2$ complex. Subsequent steps similar to the StepAD mechanism would include addition of the third strand to form the three stranded coiled coil encapsulating a linear Hg(II). Since the third strand may bind in either a parallel or antiparallel fashion, a properly folded or misfolded state can result. Our initial results, therefore, are more consistent with the dissociation mechanism; however, many further experiments are required to understand this system fully.

Conclusion

A common misconception among the protein design community has been that a highly stable peptidic scaffold is required to enforce a nonpreferred metal ion coordination environment. Therefore, significant effort is focused on designing thermodynamically favorable structures that may, by consequence of this stability, pay a significant price for the metal ion insertion. The research presented by our group[122,130] has clearly demonstrated that uncommon coordination geometries can be achieved even with relatively low peptide self-affinities. In fact, the report on the kinetic mechanism of folding of BabyL9C, TRIL9C, and GrandL9C with Hg(II) actually demonstrates that a highly stable apoprotein structure may not be kinetically optimal. It would be expected that nature would make compromises between high metal ion affinity and rapid kinetic transfer. One exciting system that may test these ideas is the metallochaperones, which traffic essential, but potentially toxic, metals from sites of uptake to utilization.

Methods

Peptide Synthesis and Purification. All peptides were synthesized on an Applied Biosystems 433A peptide synthesizer by using standard protocols[132] and purified and characterized as described.[122] The stock solution concentrations were determined by using the Ellman's test.[133]

Circular Dichroism Spectroscopy. CD titrations were performed on an AVIV 14D spectrophotometer attached to a temperature control bath. For determining association constants for the peptides in the absence of metal ions, samples containing 0, 20, 40, 50, 80, 160, 320, and 640 μM peptide in 50 mM buffer (phosphate buffer for BabyL9C, pH 8.5 and TRIS buffer for BabyL12C, pH 9.0) containing 100 mM KCl were titrated between 190 and 280 nm. The path lengths of the quartz cells were 1.0 mm for [peptide] $\geq$ 50 μM and 10 mm for [peptide] $<$50 μM.

K_{assoc} was determined by fitting $[peptide]_{folded}/[peptide]_{total}$ versus $[peptide]_{total}$ using MAPLE 7 (Waterloo Maple, Ontario, Canada).

UV−Vis Spectroscopy. Metal binding titrations of the peptides were performed by titrations of peptide into a solution containing 10 μM Hg(II) at pH 8.5 for BabyL9C and pH 9.0 for BabyL12C and monitored between 200 and 320 nm on a Carey 100 Bio UV−vis spectrophotometer attached to a temperature control bath. All solutions were purged with argon before titrations. Peptides were added from a stock solution of ~3 mM solution into a 2.5 mL solution of 10 μM $HgCl_2$ solution in 50 mM buffer (phosphate buffer, pH 8.5 for BabyL9C and Tris buffer, pH 9.0 for BabyL12C). For each addition of peptide, an equivalent addition was made in the background solution so that the difference spectra taken could be attributed only to changes due to metal−peptide conformational changes. After each addition of aliquot, the solutions were left to equilibrate for 1 min before a reading was taken. For temperature-dependent titrations, readings were taken at 10, 15, 20, 25, and 30 °C.

(132) Chan, W. C.; White, P. D. *Fmoc Solid Phase Peptide Synthesis: A Practical Approach*; Oxford University Press: New York, 2000.
(133) Ellman, G. M. *Arch. Biochem. Biophys.* **1959**, *82*, 70.

For pH titrations, between pH 4 and 10, two solutions containing 100 μM BabyL9C and 100 μM Baby12C, each containing 10 μM $HgCl_2$ solution, were monitored at the absorbance maximum for a $Hg(SR)_3^-$ LMCT band of 248 nm. The solutions were titrated between pH 4 and 10 by adding small aliquots of 1 mM solutions of potassium hydroxide and monitoring the change in pH using an Accumet gel-filled pencil-thin Ag/AgCl single-junction electrode with an Orion Research digital pH millivolt meter 611. For temperature-dependent titrations, readings were taken at 10, 15, 20, 25, and 30 °C.

Stopped Flow Spectroscopy. Stopped flow spectroscopy was performed on an Olis-RSM stopped-flow spectrophotometer monitored between 200 and 320 nm. The spectrum was observed after mixing (mixing time = 4 ms) for 1−2 s at 1000 scans/s and for 4 s and 10 s at 62 scans/s for BabyL9C and BabyL12C. For TRIL9C and TRIL12C, the spectrum was observed after mixing for 600 s and 1200 s at 1 scan/s rate. For GrandL9C, the spectrum was observed after 1 h. Reactions of 10 μM $HgCl_2$ with 100 μM peptide were performed by mixing equal volumes of 20 μM $HgCl_2$, 100 mM KCl, and 50 mM buffer (phosphate buffer pH 8.5 for BabyL9C, TRIL9C, and GrandL9C and CHES buffer pH 9.5 for BabyL12C and TRIL12C) with a solution of 200 μM peptide, 100 mM KCl, and 50 mM desired buffer. The temperatures were controlled to within ±1 °C by a Neslab Instruments (Portsmouth, NH) RTE-111 refrigerated circulating bath.

Acknowledgment. The authors thank Dr. Manolis Matzapetakis for helpful discussion and the National Institutes of Health (Grant 5 R01 ES012236-02) for funding the research work conducted.

IC048939Z